

Depinning Transition in the Failure of Inhomogeneous Brittle Materials

Laurent Ponson*

*Graduate Aerospace Laboratories (GALCIT), California Institute of Technology, Pasadena, California 91125, USA
Program of Civil Engineering, COPPE/Universidade Federal do Rio de Janeiro, CEP 21945-970 RJ, Rio de Janeiro, Brazil
(Received 12 July 2008; published 27 July 2009)*

The dynamics of cracks propagating in elastic inhomogeneous materials is investigated experimentally. The variations of the average crack velocity with the external driving force are measured for a brittle rock and shown to display two distinct regimes: an exponential law characteristic of subcritical propagation at a low driving force and a power law above a critical threshold. This behavior can be explained quantitatively by extending linear elastic fracture mechanics to disordered systems. In this description, the motion of a crack is analogous to the one of an elastic line driven in a random medium, and critical failure occurs when the external force is sufficiently large to depin the crack front from the heterogeneities of the material.

DOI: 10.1103/PhysRevLett.103.055501

PACS numbers: 62.20.mm, 46.50.+a, 68.35.Ct

The failure of inhomogeneous materials has been a very active field of research during the past decades (see Ref. [1] for a recent review). A great deal of research effort in this field has been dedicated to the study of fluctuations: fluctuations of velocity around the average motion of cracks when the studies were devoted to their highly intermittent dynamics [2,3] or variations to a straight trajectory when the works were dedicated to the rough geometry of fracture surfaces [4]. In both cases, these fluctuations were shown to display remarkably robust properties suggesting that crack propagation in disordered systems could be described in a general manner by relatively simple statistical models able to capture the competition between the two antagonist effects occurring during the failure of inhomogeneous materials: disorder and elasticity.

Very recently, the main statistical features of the fluctuations of both the trajectory and velocity for cracks propagating in brittle materials were captured by stochastic models of elastic lines driven in random media [5,6] that mimic the motion of cracks through the microstructural disorder of materials. However, the relevance of this theoretical framework for fracture problems is still a matter of debate: On the one hand, the ability of these models to describe the *average behavior* of the crack such as its mean velocity, or the critical external loading at failure, more interesting from a mechanical or an engineering point of view, is still an open question. On the other hand, a direct experimental observation of the critical dynamic transition from a crack pinned by the heterogeneities of the material ($v = 0$) to a propagating crack ($v > 0$) as predicted by this theory at the onset of material failure (driving force $G = G_c$) is still lacking. The investigation of this depinning transition on an experimental example is the central point of this Letter.

The variations of the average crack velocity with the external driving force or elastic energy release rate G are measured for a brittle rock. They are shown to exhibit two

distinct regimes, characteristic of a thermally activated process below the threshold G_c , and a critical failure at larger driving force $G > G_c$. This behavior is fully captured by a stochastic model rigorously derived from fracture mechanics extended to inhomogeneous systems where crack propagation is analogous to the motion of an elastic line driven in a random medium.

System and setup.—Sandstone is chosen as an archetype of heterogeneous elastic materials. A Botucatu sandstone, extracted in the central region of Brazil, has been used for the experiments. It is made of quartz grains with a diameter $d = 230 \pm 30 \mu\text{m}$ and a porosity $\phi = 17 \pm 2\%$, that results in highly inhomogeneous mechanical properties at the grain scale. This South American rock is consolidated thanks to an iron oxide cement providing to the rock a red coloration. As a result, its fracture energy $G_c \approx 140 \text{ J m}^{-2}$ as measured in the following is relatively high compared to other sandstones [7]. Its intrinsic tensile strength measured by splitting cylinders submitted to uniaxial compression [8] is found to be $\sigma_Y = 75 \pm 20 \text{ MPa}$, while its Young's modulus is found to be $E = 25 \pm 1 \text{ GPa}$. This leads to an estimate of the size of the process zone next to the crack tip where damage and dissipative pro-

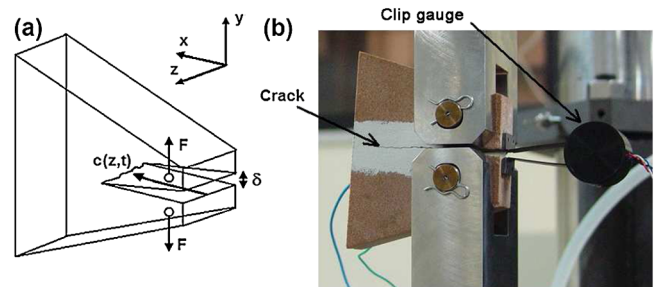


FIG. 1 (color online). Experimental setup. (a) Sketch of the tapered double cantilever beam geometry; (b) picture of the specimen during crack propagation.

cesses are localized: $\ell_{PZ} = \frac{\pi}{8} \frac{GcE}{\sigma_y} \approx 250 \mu\text{m}$ [9]. The comparison with the grain size $d \approx \ell_{PZ}$ suggests that crack propagation in the Botucatu rock can almost be assimilated to the motion of a crack in an ideal *brittle* material where the quartz grains play the role of the basic microstructural feature.

A new experimental setup has been developed in order to measure variations of crack velocity from slow to very fast propagation in brittle materials. Contrary to the torsion tests classically used to measure the $v(G)$ curves in rocks [7,10], the tapered double cantilever beam specimens used in the experiments [Fig. 1(a)] result in a slight and controlled acceleration of the crack produced by the tapered shape of the samples. As a consequence, it is possible to measure crack velocities up to $v \approx 1 \text{ m s}^{-1}$ not achieved by classical fracture tests. In addition, the external tensile loading produces relatively straight crack fronts, allowing a simple interpretation of the experiments. Finally, a straight crack propagation is obtained without lateral guide grooves that produce generally a large scattering of the experimental $v(G)$ curves [10].

An initial notch $c_0 = 35 \text{ mm}$ is machined in 100 mm long samples with thickness $e = 30 \text{ mm}$. They are submitted to a uniaxial traction by increasing the displacement $\delta_F = v_{\text{ext}} t$ at the velocity $0.2 \mu\text{m s}^{-1} \leq v_{\text{ext}} \leq 4 \mu\text{m s}^{-1}$ between two rods previously inserted in the drilled specimens. The experiments are performed at room temperature with a humidity of $75\% \pm 5\%$. During the test, a force gauge measures the applied tension F while a clip gauge measures the opening displacement δ between the two lips of the crack with a precision of 100 nm [see Fig. 1(b)]. A typical force-crack opening displacement curve obtained during a fracture test of a Botucatu specimen is presented in Fig. 2.

The initial linear part of the curve—prior crack initiation—allows for an estimation of the Young's modulus $E = 25 \pm 1 \text{ GPa}$ of the sandstone, in agreement with the

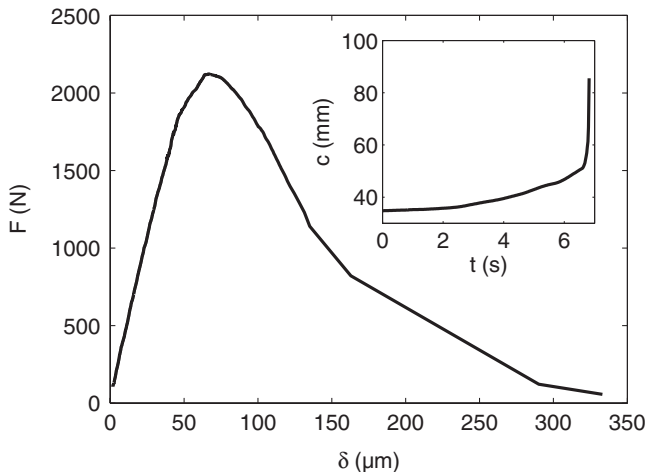


FIG. 2. Mechanical behavior of the specimen. Typical load-crack opening displacement curve; (inset) corresponding evolution of the average position of the crack front.

value obtained from the measurement of its compressive and shear wave speeds. After crack initiation, the average position of the crack front $c = \langle c(z) \rangle_z$ is measured using finite element (FE) simulations of an elastic specimen in the same geometry: We run several simulations with various values of the crack length c to measure the variations of the specimen compliance $\lambda^{\text{FE}}(c)$. This function is then compared to the experimental compliance $\lambda(t) = \delta/F$ in order to measure the crack length $c(t)$ at each time step t . The variations of $c(t)$ obtained by this method are represented in inset in Fig. 2. To validate our approach, we have also measured the position of the crack tip at the sample free surface using two other techniques: The increase in resistance of a thin conductive film deposited on the sample side (potential drop method) is related to c , while snapshots of the propagating crack observed from the side of the sample are recorded and analyzed. Both methods confirm the results obtained from the FE-based technique, providing, however, less precise measurements.

From the evolution of the crack length, it is now possible to measure the crack speed $v = \frac{dc}{dt}$ as well as the driving force G imposed to the system during the test. Using the load-displacement curve to measure the work δW of the tensile machine during the span δt , one gets $G(t) = \frac{\delta W(t)}{e[c(t+\delta t) - c(t)]}$ [11]. On the other hand, the driving force is estimated independently using the relation $G(t) = [F(t)]^2 g^{\text{FE}}[c(t)]$, where the geometrical part g^{FE} of the energy release rate is provided by the FE simulations. Both methods lead to similar results within 2%.

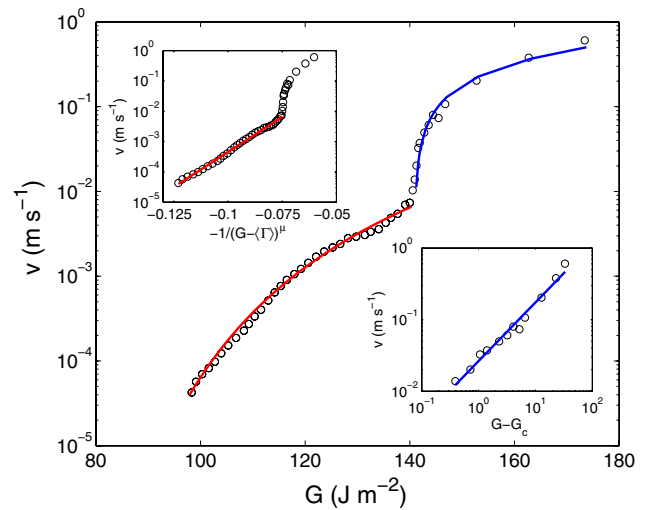


FIG. 3 (color online). Average dynamics of a crack propagating in Botucatu sandstone. The variations of the crack velocity are plotted in logarithmic scale with respect to the crack driving force. The subcritical regime $G < G_c$, with $G_c = 140 \text{ J m}^{-2}$, is studied in the top-left inset. The solid line corresponds to the best fit of the data in $v \sim e^{-C/(G-G_c)^\mu}$, with $\mu = 0.60$ obtained for $\langle \Gamma \rangle = 65 \text{ J m}^{-2}$. The bottom right inset shows the velocity variations with the net loading $G - G_c$ in a logarithm representation for $G > G_c$. The straight line corresponds to a power law fit with exponent $\theta = 0.80$.

Experimental results.—The variations of the crack velocity with the driving force as observed on the sandstone specimens are represented in Fig. 3 in semilogarithmic coordinates. Velocity measurements are achieved over almost 5 orders of magnitude, corresponding to a relatively small variation of the driving force. Irrespective of the external loading rate v_{ext} , the failure behavior of the rock is found to be systematically characterized by two very different regimes defining G_c . Near but above this critical loading, a slight change in the driving force results in a strong variation in the crack velocity. This high sensitivity is studied in more detail in the bottom right inset in Fig. 3, where v is plotted as a function of the net driving force $G - G_c$ in logarithmic coordinates. The linear behavior in this representation suggests a power law variation of the crack velocity $v \sim (G - G_c)^\theta$, with $G_c = 140 \pm 3 \text{ J m}^{-2}$ and $\theta = 0.80 \pm 0.15$.

The variations of velocity at driving forces $G < G_c$ are now studied. Contrary to the previous regime, slow crack propagation in rocks has been largely investigated and shown to depend crucially on the temperature [7,10]. Analytical forms such as $v \sim e^{-(E^*/k_B T)} G^{n/2}$ [12] or $v \sim e^{-(E_0 - bG)/k_B T}$ [13] are usually used to describe the experimental data. Both formulas reproduce correctly the measurements reported here as far as $G < 120 \text{ J m}^{-2}$. The first one, largely used because of its rather simple and compact form characterized by one subcritical crack growth index, leads to $n \simeq 34$ that compares well with the other experimental findings for sandstone [7]. The second formula leads to $b \simeq 0.68 \times 10^{-20} \text{ m}^2$, which is also in agreement with the other measurements made on rocks with a similar microstructure [10]. This last description is based on the Arrhenius law $v \sim e^{-(E_a/k_B T)}$, where the activation energy $E_a = E_0 - bG$ represents the typical barrier along the energy landscape tilted by the external force G . Thus, large values of G corresponding to high tensile forces increase the probability of bond rupture by thermal activated processes, such as, e.g., thermal stress fluctuations [14] and chemical reactions [15]. However, this theoretical approach supposes that the typical energy barrier remains independent of the geometry of the crack front. This assumption is perfectly fair as far as one considers the motion of a crack tip in a 2D medium, but, in the more realistic situation of a 3D inhomogeneous material, the crack line can take advantage of the material elasticity to deform and explore an energy landscape rather different from the raw fluctuations produced by the material heterogeneities. In this context, one can show that $E_a \sim (G - \langle \Gamma \rangle)^{-\mu}$, with $\mu \simeq 0.60$ as justified in the next section. The Arrhenius law $v \sim e^{-(E_a/k_B T)}$ provides then a good description of the experimental data for the full subcritical regime $G < G_c$ as shown in Fig. 3. The upper left inset represents the best fit obtained for $\langle \Gamma \rangle = 65 \pm 5 \text{ J m}^{-2}$.

Discussion.—The observation of two very different regimes with an exponential variation of v with the external driving force for $G < G_c$ and a power law behavior for

$G > G_c$ reveals a fundamental aspect of the dynamics of cracks propagating in brittle inhomogeneous media. Let us derive an equation of motion for the crack to understand more quantitatively this behavior. As a starting point, we assume that the local velocity $v(M)$ of a point M along the crack front is proportional to the excess of energy $G(M) - \Gamma(M)$ locally released by the system, where Γ refers to the local fracture energy. This corresponds to a damped dynamics where the inertial effects are neglected. In a disordered material such as sandstone, the fracture energy can be described as a stochastic field $\Gamma(M) = \langle \Gamma \rangle + \delta\Gamma\eta(M)$, where η is a short range correlated random term with zero mean value and unit second order moment. These material heterogeneities induce perturbations of the crack front—parallel in average to the z axis and propagating along the x axis—both in the mean fracture plane (x, z) [in-plane perturbations $c(z, t) - \langle c(z, t) \rangle_z$] and in the perpendicular direction y [out-of-plane perturbations $h(z, t)$]. They in turn lead to variations in the local value of the external driving force $G(M)$. Interestingly, for small perturbations, $G(M)$ depends only on the in-plane deviations of the crack front [16] and is given by $G(z, t) = G + \frac{G}{\pi} \int_{-\infty}^{\infty} \frac{c(z', t) - c(z, t)}{(z' - z)^2} dz'$ [17], where G refers to the macroscopic driving force applied by the tensile machine to the specimen. Using the previous expressions of the local driving force and fracture energy, one gets the equation of motion for a crack front propagating in a 3D brittle inhomogeneous material:

$$\frac{\partial c}{\partial t} \Big|_{z,t} \sim (G - \langle \Gamma \rangle) + \frac{G}{\pi} \int_{-\infty}^{\infty} \frac{c(z', t) - c(z, t)}{(z' - z)^2} dz' + \delta\Gamma\eta(c, h, z). \quad (1)$$

As the out-of-plane perturbations h behave independently of c , the stochastic term in Eq. (1) is analogous to a 2D random potential depending only on c and z . Therefore, the crack motion is described by an equation of pinning of an elastic line driven in a random medium comparable to the one proposed in the context of interfacial cracks propagating in inhomogeneous weak planes [18]: If the driving force G exceeds the threshold

$$G_c \simeq \langle \Gamma \rangle + \pi(\delta\Gamma)^2/\langle \Gamma \rangle, \quad (2)$$

the crack propagates, while the front is pinned by the material heterogeneities if $G < G_c$ [19]. Note that the effective fracture energy G_c is larger than the average value $\langle \Gamma \rangle$ of the local fracture energy. Above the threshold, the mean velocity v of the crack front is expected to scale as $(G - G_c)^\theta$, where θ is called the velocity exponent. Equation (1) has been studied using functional renormalization group techniques [20,21], providing $\theta = 0.78$ and $\theta = 0.59$ to first and second order in perturbation, respectively. Recent direct numerical simulations resulted in $\theta \simeq 0.63$ [22]. As a consequence, the power law behavior measured experimentally with exponent $\theta \simeq 0.80$ suggests that a *depinning transition* from a pinned to a moving crack as described in Eq. (1) occurs at $G = G_c$. Note that such an

interpretation of the failure of inhomogeneous materials had already been suggested by experiments made on other kinds of materials for which damage processes play a crucial role, preventing a quantitative comparison with the predictions of linear elastic fracture mechanics [23].

Below the threshold at zero temperature, the external driving force is too low, and the crack front is pinned by the material heterogeneities. However, at room temperature, thermally activated processes can enable a subcritical propagation. In this regime, described by adding an annealed noise $\eta_T(z, t)$ to Eq. (1), one expects also a collective motion of the line characteristic of glassy systems, and the velocity is given by $v \sim e^{-(\ell/\pi)^{1+\mu}[\langle\Gamma\rangle^{1+\mu}/k_B T(G-\langle\Gamma\rangle)^\mu]}$, where $\mu \approx 0.60$ for long-range elasticity [24]. This so-called creep law, first proposed for the subcritical crack dynamics in Ref. [25] and then observed in the context of paper peeling [3], describes rather well the experimental measurements presented here over the whole range of subcritical loadings $G < G_c$. This leads to activation energies in the range $E_a = \frac{\ell^2}{\pi^{1+\mu}} \frac{\langle\Gamma\rangle^{1+\mu}}{(G-\langle\Gamma\rangle)^\mu} \approx 0.20\text{--}0.35$ eV, 1 order of magnitude larger than the thermal energy $k_B T$. Interestingly, this expression provides an estimate of the toposity—size of the basic feature of the perturbed crack front— $\ell \approx 0.1$ nm, compatible with the interatomic distance. This suggests that thermally activated crack propagation and critical failure might involve processes defined at two very different length scales: atomic and grain size, respectively. Finally, let us note that using Eq. (2), the experimental values of the critical driving force G_c and the average fracture energy $\langle\Gamma\rangle$ allow one to estimate the normalized fluctuations $\frac{\delta\Gamma}{\langle\Gamma\rangle} = \sqrt{(G_c - \langle\Gamma\rangle)/\pi\langle\Gamma\rangle} = 0.61 \pm 0.04$ of fracture energy in the Botucatu rock, slightly larger but comparable with an estimate of this quantity $\sqrt{\phi/(1-\phi)} \approx 0.5$ for an ideal porous material made of an homogeneous solid with constant fracture energy and voids, with volume fractions $1 - \phi = 0.83$ and $\phi = 0.17$, respectively.

Conclusion.—The average dynamics of a crack propagating in a brittle inhomogeneous rock has been experimentally investigated. The velocity variations with the crack driving force display two very different regimes: Above a threshold G_c , v evolves as a power law $(G - G_c)^\theta$ with exponent $\theta = 0.80 \pm 0.15$, while for $G < G_c$, these variations are described by an Arrhenius law $v \sim e^{-(E_a/k_B T)}$ with typical energy barriers $E_a \sim (G - \langle\Gamma\rangle)^{-\mu}$, where $\mu \approx 0.60$. This behavior can be quantitatively explained by extending fracture mechanics to disordered systems. In this description, the resistance to failure of a material is interpreted as the critical force to depin the crack front from the material heterogeneities. Below this depinning transition, the line can also propagate, but at much smaller velocities through thermal activated processes, and the velocity variations are provided by a creep law as observed experimentally. The experimental results presented here and their theoretical interpretation open

new perspectives for the prediction of macroscopic quantities of direct interest for engineering and applied science. They make the link between the microstructural properties of a brittle material and its fracture energy or the crack velocity. This bridge might help to design stronger materials with increased lifetimes.

The author thanks G. C. Cordeiro and A. Bindal for their help in the experiments and M. Alava, K. Bhattacharya, D. Bonamy, E. Bouchaud, J.-B. Leblond, S. Morel, A. Rosso, and R. Toledo for helpful discussions. Financial support from the French Ministry of Foreign Affairs through the Lavoisier Program is acknowledged.

*ponson@caltech.edu

- [1] M. J. Alava, P. K. Nukala, and S. Zapperi, *Adv. Phys.* **55**, 349 (2006).
- [2] K. J. Måløy and J. Schmittbuhl, *Phys. Rev. Lett.* **87**, 105502 (2001); K. J. Måløy, S. Santucci, J. Schmittbuhl, and R. Toussaint, *Phys. Rev. Lett.* **96**, 045501 (2006);
- [3] J. Koivisto *et al.*, *Phys. Rev. Lett.* **99**, 145504 (2007).
- [4] E. Bouchaud *et al.*, *Europhys. Lett.* **13**, 73 (1990); K. J. Måløy *et al.*, *Phys. Rev. Lett.* **68**, 213 (1992); L. Ponson *et al.*, *Phys. Rev. Lett.* **96**, 035506 (2006).
- [5] D. Bonamy *et al.*, *Phys. Rev. Lett.* **97**, 135504 (2006).
- [6] D. Bonamy, S. Santucci, and L. Ponson, *Phys. Rev. Lett.* **101**, 045501 (2008).
- [7] B. K. Atkinson, *J. Geophys. Res.* **89**, 4077 (1984).
- [8] F. L. L. B. Carneiro and A. Barcellos, *Bull. RILEM* **13**, 97 (1953).
- [9] G. I. Barenblatt, *Adv. Appl. Mech.* **7**, 55 (1962).
- [10] Y. Nara and K. Kaneko, *Int. J. Rock Mech. Min. Sci. Geomech. Abstr.* **42**, 521 (2005).
- [11] S. Morel *et al.*, *Int. J. Fract.* **131**, 385 (2005).
- [12] R. J. Charles, *J. Appl. Phys.* **29**, 1554 (1958).
- [13] S. M. Wiederhorn *et al.*, *J. Am. Ceram. Soc.* **57**, 336 (1974).
- [14] S. Santucci *et al.*, *Phys. Rev. Lett.* **93**, 095505 (2004).
- [15] S. M. Wiederhorn, *J. Am. Ceram. Soc.* **50**, 407 (1967).
- [16] R. C. Ball and H. Larralde, *Int. J. Fract.* **71**, 365 (1995); A. B. Movchan, H. Gao, and J. R. Willis, *Int. J. Solids Struct.* **35**, 3419 (1998).
- [17] J. R. Rice, *J. Appl. Mech.* **52**, 571 (1985).
- [18] J. Schmittbuhl *et al.*, *Phys. Rev. Lett.* **74**, 1787 (1995); S. Ramanathan *et al.*, *Phys. Rev. Lett.* **79**, 873 (1997).
- [19] A. L. Barabási and H. E. Stanley, *Fractal Concepts in Surface Growth* (Cambridge University Press, Cambridge, England, 1995).
- [20] D. Ertas and M. Kardar, *Phys. Rev. E* **49**, R2532 (1994).
- [21] P. Chauve *et al.*, *Phys. Rev. Lett.* **86**, 1785 (2001).
- [22] O. Duemmer and W. Krauth, *J. Stat. Mech.* (2007) P01019.
- [23] P. Daguiet *et al.*, *Phys. Rev. Lett.* **78**, 1062 (1997).
- [24] M. V. Feigelman *et al.*, *Phys. Rev. Lett.* **63**, 2303 (1989); P. Le Doussal *et al.*, *Phys. Rev. E* **69**, 026112 (2004); A. B. Kolton *et al.*, *Phys. Rev. Lett.* **94**, 047002 (2005).
- [25] L. Ponson *et al.*, in *Proceedings of FRAMCOS-6, Catania, Italy*, edited by A. Carpinteri *et al.* (Taylor & Francis, London, 2007), p. 63.